

Ion Polymer Interactions in DNA Solutions and Gels

Ferenc Horkay

Summary: Systematic investigations using small angle neutron scattering (SANS) were made to reveal the effect of calcium ions on the structure of DNA gels and solutions in near-physiological salt solutions. To describe the neutron scattering response two characteristic distances are required. The shorter length scale, R (≈ 10 Å), was found to be governed by the geometry of the DNA chain and is close to the cross-sectional radius of the double helix. The longer length scale L corresponds to the mesh size of the network of overlapping polymer chains. L decreases with increasing DNA concentration as $L \propto c_{DNA}^{-0.73}$. With increasing CaCl_2 concentration both L and the scattering intensity increase. The increase in the scattering intensity reflects the reduction of the osmotic modulus as the calcium ion concentration increases. The values of the osmotic modulus derived from osmotic swelling pressure measurements are in reasonable agreement with those obtained from SANS.

Keywords: calcium ion; DNA; osmotic pressure; polyelectrolyte; small angle neutron scattering; swelling

Introduction

The interactions of DNA with small ions are of importance in a variety of scientific areas. In the presence of multivalent cations (e.g., spermine, spermidine, polyamines) DNA forms compact structures, such as spherical nanoparticles, rods or toroids.^[1–5] In gene therapy DNA containing genes are transferred from solution into the target cells.^[6,7] Understanding interactions between DNA and various cations is essential to design and control the properties (e.g., size, compactness, stability) of DNA-based nanomedicines. The biological activity of the nanomedicine depends on the competing requirements of having sufficient stability to escape endosomal degradation after cellular uptake and to remain intact all the way upon to arrive in the nucleus where the function of the nanoparticle requires unraveling and releasing the DNA to

achieve gene expression.^[8–10] It is important to note that DNA condensation is not sensitive to the chemistry (e.g., base pair sequence) of the DNA, i.e., fitting DNA into small packages only weakly depends on the genetic code.

Relatively little attention has been paid to the effect of divalent counterions on the conformation of DNA. Unlike multivalent cations of charge +3 or more calcium ions do not cause DNA condensation but induce reversible conformational changes. For example, it is known that submillimolar levels of calcium regulate DNA conformation at the $d(\text{TG/AC})_n$ repeat, which is a frequent dinucleotide repeat of the mammalian genome.^[11,12] It is thought that this conformational change provides the genome with flexibility permitting far-distant DNA interactions, and it may also affect protein-DNA interactions. However, the effect of calcium ions on the larger scale structure of the DNA molecule has not yet been fully explored.

Most solution properties of charged polymer molecules are affected by the distribution of small ions in the neighborhood

Section on Tissue Biophysics and Biomimetics, NICHD, National Institutes of Health, 13 South Drive, Bethesda, MD, 20892, USA
E-mail: horkayf@helix.nih.gov

of their macroion.^[13,14] In the case of strong coupling, counterions are assembled around the polyion. For locally rod-like polymers, such as DNA, the distribution of monovalent counterions can be reasonably well described by the Poisson-Boltzmann theory.^[15] However, this model breaks down when the electrostatic interactions involve higher valence counterions.^[16,17] Recent anomalous small-angle X-ray scattering (ASAXS) studies show that divalent counterions prefer to stay in the vicinity of the oppositely charged polymer chains. These ions are not localized but can move along the chain.^[18–20]

The understanding of the effect of multivalent ions on the organization of polyelectrolyte molecules in solution has significantly progressed, owing to advances in the field of molecular dynamics simulations.^[21–23] It has been shown, for instance, that in these systems a net attractive interaction occurs between like charged macroions and they can attract each other due to charge fluctuations in the counterion distribution. In the presence of divalent counterions, stiff polyelectrolyte chains may spontaneously form bundles.^[21] With long flexible chains, aggregation can occur, but bundles do not form.^[22] For monovalent counterions, aggregation is absent. Systematic experimental observations to quantify the effect of ions on the organization of polyelectrolyte molecules at higher concentration (i.e., in the semi-dilute concentration range), however, are lacking. Such measurements can contribute to a better understanding of polyion-small ion interactions and is essential to control structure and stability of DNA in the biological milieu.

In this work we investigate the effect of calcium ions on the structure and thermodynamic properties of DNA solutions and gels in near-physiological salt solutions. The concentration of DNA at constant salt content and the concentration of calcium ions at constant DNA content are varied. Small angle neutron scattering (SANS) is used to explore ion induced changes in the organization of DNA molecules over a wide

length scale range $0.003 \text{ \AA}^{-1} < q < 0.2 \text{ \AA}^{-1}$, where q is the scattering wave vector [$q = (4\pi/\lambda)\sin(\theta/2)$, θ being the scattering angle and λ is the wavelength of the incident neutrons].

Scattering from Macromolecular

Solutions

Binary solutions of neutral polymers consist of a polymer component and a low molecular weight solvent. The scattering properties of semi-dilute flexible polymer solutions^[24] are described by a correlation length ξ that defines the average spatial extent of the thermal concentration fluctuations and is the result of short range Van der Waals interactions. The correlation length is related to the mesh size of the overlapping macromolecules and can be measured by small angle scattering techniques. In the case of random thermal concentration fluctuations, the scattering response is described by the Ornstein-Zernike function^[24,25]

$$I_{\text{dyn}}(q) = \Delta\rho^2 \frac{k_B T \varphi}{\partial\Pi/\partial\varphi} \frac{1}{(1 + q^2 \xi^2)} \quad (1)$$

where $\Delta\rho^2$ is the contrast factor between polymer and solvent, k_B is the Boltzmann constant, T is the absolute temperature, Π is the osmotic pressure of the polymer solution, and φ is the volume fraction of the polymer.

When the polymer chain contains rigid segments eq. 1 has to be modified. In this case the scattering intensity varies as $1/q$. We consider a system containing linear segments of finite cross-sectional radius R . At sufficiently high concentrations the polymer molecules overlap and form a network of mesh size L . This distance is expected to decrease with increasing polymer concentration. The following expression, which is valid in the Guinier region $qR < 1$, has been found to describe the scattering response of semidilute polysaccharide solutions^[26]

$$I_{\text{dyn}}(q) = \Delta\rho^2 \frac{k_B T \varphi}{\partial\Pi/\partial\varphi} (1 + q^2 L^2)^{-1/2} \times (1 + q^2 R^2)^{-1} \quad (2)$$

For DNA, the cross-sectional radius $R \approx 10 \text{ \AA}$.

In polymer solutions in which molecular associations or other large-scale structures are present, the description of the scattering response requires an additional (static) term. Polyelectrolyte solutions develop such molecular associations owing to hydrophobic interactions in the polymer backbone. These features give rise to an extra contribution at small angles, which takes the form of a power law

$$I_{\text{stat}}(q) = Aq^{-m} \quad (3)$$

where $m = 4$ in the case of smooth surfaces (Porod scattering).^[27] Increasing the surface roughness is reflected in a lower value of m .^[28] The total scattering intensity thus takes the form

$$\begin{aligned} I(q) &= I_{\text{dyn}}(q) + I_{\text{stat}}(q) \\ &= \Delta\rho^2 \frac{k_B T \varphi}{\partial \Pi / \partial \varphi} \left[(1 + qL)^2 \right]^{-1/2} \\ &\quad (1 + q^2 R^2)^{-1} + Aq^{-m} \end{aligned} \quad (4)$$

Experimental Part

Sample Preparation

DNA solutions were made from sodium salt of double-stranded DNA (Sigma, salmon testes, $M_w = 1.3 \cdot 10^6$) in 100 mM NaCl solution. The percentage of G-C content was 41.2%. The concentrations of the DNA solutions were 1%, 2%, 3% and 6% w/w.

Gels were prepared by crosslinking DNA solutions with ethyleneglycol diglycidyl ether (2%) at pH = 9.0 using tetramethylethylenediamine (TEMED) to adjust the pH.^[29] Crosslinks were introduced at 3% and 6% w/w DNA concentrations. After gelation, the gels were washed with deionized water, and swollen in 100 mM NaCl solution (nearly physiological condition). The concentration of the CaCl_2 in the equilibrium NaCl solution was gradually increased from zero to 0.8 mM. At greater CaCl_2 concentration volume

transition occurs in the present system. All measurements were performed below this threshold concentration.

Small Angle Neutron Scattering

Measurements

SANS measurements were made on the NG3 instrument at NIST, Gaithersburg MD. The temperature during the experiments was maintained at $25.0 \pm 0.1 \text{ }^\circ\text{C}$. The solutions were prepared in D_2O . Measurements were carried out at two sample-detector distances, 2.5 m and 13.1 m, with incident wavelength 8 \AA . After radial averaging, corrections for incoherent background, detector response and cell window scattering were applied. The intensity normalization was made with NIST standard samples.^[30]

Osmotic Pressure Measurements

DNA gels were equilibrated with poly(vinyl pyrrolidone) solutions (molecular weight: 29 kDa) of known osmotic pressure using a dialysis bag to prevent penetration of the polymer into the network.^[31,32] When equilibrium was reached, the concentration of both phases was measured. This procedure yields the dependence of Π upon the polymer volume fraction, φ , for each gel.

Elastic Modulus Measurements

The shear moduli of the DNA gels were determined by a TA.XT2I HR texture analyzer (Stable Micro Systems, U.K.). Uniaxial compression measurements were made on cylindrical gel specimens (height = diameter $\approx 1 \text{ cm}$). Equilibrated gel samples were rapidly transferred from the dialysis bag into the apparatus, which measures the compressive deformation (precision: $\pm 0.001 \text{ mm}$) as a function of an applied force (precision: $\pm 0.01 \text{ N}$). The absence of sample volume change and barrel distortion was confirmed, and the stress-strain isotherms were analyzed using the relation

$$\sigma = G \Lambda - \Lambda^{-2} \quad (5)$$

where σ is the nominal stress (force per unit undeformed cross-section), G is the shear modulus and Λ is the deformation ratio.^[33] The stress–strain data were determined in the range of deformation ratio $0.7 < \Lambda < 1$.

All measurements were carried out at $25.0 \pm 0.1^\circ\text{C}$ and at $\text{pH} = 7$.

Results and Discussion

Figure 1a shows the SANS spectra for solutions prepared with different DNA concentrations in 100 mM NaCl. For clarity, the intensity of each successive curve is shifted by a factor of 10 with increasing DNA concentration. All the scattering curves exhibit the same general features. The power law behavior observed at low values of q ($< 0.08 \text{ \AA}^{-1}$) is characteristic of scattering of large clusters.^[34–37] Because of the absence of a characteristic length scale, such as a shoulder, the size of the clusters is not resolved in the SANS measurements. At low values of q the slope varies in the range $3.1 < m < 3.4$. Such a power-law scattering is indicative of the fractal-like behavior of the system. For scattering from objects with fractal surface, the power law exponent is $-(6-D_s)$, where D_s is the fractal

dimension ($2 < D_s < 3$). $D_s = 2$ represents a smooth surface. The slope of the log-log plot in Figure 1a yields $2.6 < D_s < 2.9$.

At intermediate q a plateau region is distinguishable, which is described by the first term in eq 4. The continuous curves through the data points are the least squares fits to eq. 4.

Figure 1b shows the values of L and R obtained from the fits. The mesh size L decreases with increasing DNA concentration, with a slope of approximately -0.73 in the double logarithmic representation. This behavior can be attributed to increasing overlap of the DNA strands with increasing overall polymer concentration. It may be recalled that, in scaling theory,^[24] the expected exponent for overlapping flexible polymer chains in excluded volume conditions is $-3/4$.

In Figure 2 the SANS curves of two DNA gels are compared with those of the corresponding uncrosslinked DNA solutions. The scattered intensity from the gels exceeds that from the solutions. The scattering curves of both the gels and solutions can be reasonably well described by eq. 4. The values of L and R obtained from the fits show that L is greater in the gel than in the corresponding solution by

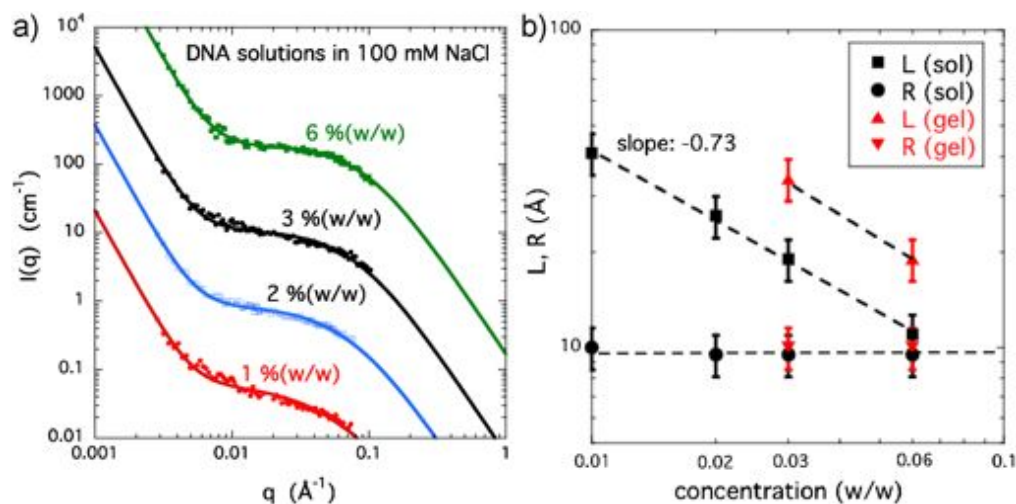


Figure 1.

a. SANS spectra of DNA solutions with $c_{\text{DNA}} = 1, 2, 3, 6\%$ w/w in 100 mM NaCl. Each curve is multiplied by a factor of 10 with respect to the previous lower DNA concentration. b. Dependence of L and R on DNA concentration in 100 mM NaCl. The triangles show the corresponding data for DNA gels at 3% and 6% w/w.

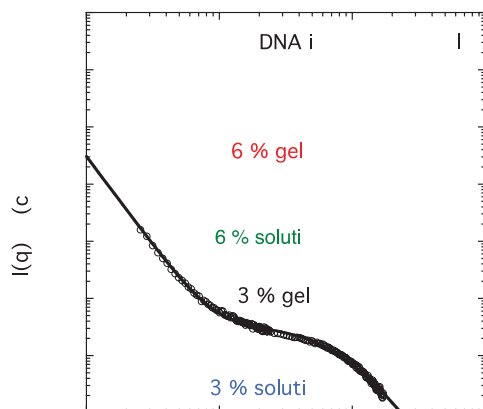


Figure 2.

SANS curves for DNA solutions and gels. The continuous curves through the data points are the least squares fits of eq. 4.

approximately 50% (Figure 1.b). This finding is consistent with the increased heterogeneity of the crosslinked systems.

Figure 3a shows the SANS spectra of a 6% DNA gel swollen in 100 mM NaCl solutions with different calcium chloride concentrations. In polyelectrolyte solutions and gels higher valence counterions adsorb on the polymer backbone (Manning

condensation^[38]). These ions may form stable multiplet structures in which they are shared between negatively charged groups of the same or different macroanion. The attractive interaction between neighboring chains favors molecular association and leads to the formation of bundles or branched structures. It is important to note that alkaline earth metal ions are reversibly associated with DNA chains, i.e., structure formation in solution is an equilibrium process.

At low q , the lack of significant change in intensity implies that calcium ions only slightly affect the clusters. This finding suggests that clustering is primarily caused by hydrophobic interactions rather than electrostatic attraction between the DNA strands. At intermediate length scales, however, the scattering intensity is significantly enhanced and the slope becomes steeper. In spite of the highly overlapping condition of the DNA strands, for the gel with the highest CaCl_2 content the region in which the scattering intensity varies as q^{-1} is clearly distinguishable. The shoulder (around $q \approx 0.1 \text{ \AA}^{-1}$) is shifted towards lower values of q as the CaCl_2 concentration increases. At the highest values of q all the curves tend to coincide, i.e., the local

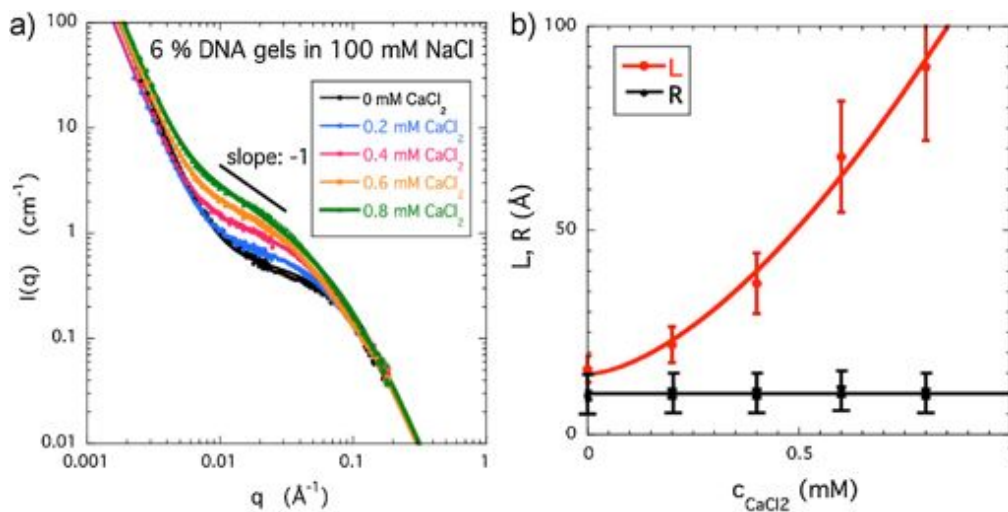


Figure 3.

a. SANS response of 6% w/w DNA gels swollen in 100 mM NaCl solution containing different amounts of CaCl_2 . The continuous curves through the data points are the least squares fits of eq. 4. b shows the variation of L and R as a function of the CaCl_2 concentration in the equilibrium solution.

chain geometry is not influenced by the calcium ions.

The continuous lines through the data points in Figure 3a are the least squares fits of eq. 4. The parameters obtained from the fits for L , R , m and $I_{\text{dyn}}(0)$ are listed in Table 1. It can be seen that both L and the intensity of the thermodynamic concentration fluctuations $I_{\text{dyn}}(0)$ increase with increasing calcium chloride concentration. The mesh size L increases strongly with the calcium ion content, tending towards the persistence length of the DNA ($\approx 500 \text{ \AA}$). This finding is consistent with the general behavior of phase separating polymer solutions, where the spatial range of the thermodynamic concentration fluctuations increases as the transition is approached.^[24] It can also be seen that R is practically independent of the calcium chloride concentration.

In the intermediate q range the scattering intensity gradually increases with increasing calcium chloride content as the volume transition is approached. Since in this region the scattering intensity is of thermodynamic origin, its enhancement extends to the thermodynamic limit ($q \rightarrow 0$), where $I_{\text{dyn}}(0)$ is defined by

$$I_{\text{dyn}}(0) = \frac{\Delta\rho^2 k_B T \varphi}{(\partial\Pi/\partial\varphi)} \quad (6)$$

The increased intensity reflects the decrease of $\partial\Pi/\partial\varphi$ with increasing calcium chloride concentration.

To confirm this picture we determined $I_{\text{dyn}}(0)$ of the DNA gels from osmotic swelling pressure measurements and shear modulus measurements. The osmotic pressure Π_{cr} of the crosslinked DNA was

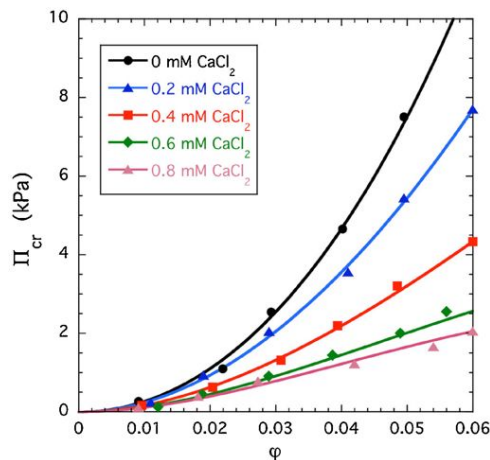


Figure 4. Osmotic pressure Π_{cr} versus DNA volume fraction φ for gels swollen in 100 mM NaCl solution containing different amounts of CaCl_2 .

estimated from eq. 7

$$\Pi_{\text{cr}} = \Pi_{\text{sw}} + G \quad (7)$$

where Π_{sw} is the swelling pressure and G is the shear modulus of the gel.

The effect of calcium chloride concentration on Π_{cr} is illustrated in Figure 4. The results show that Π_{cr} gradually decreases with increasing calcium chloride concentration. Addition of 0.8 mM CaCl_2 reduces Π_{cr} by almost an order of magnitude. At the phase transition the osmotic pressure vanishes.

The scattering intensity at $q = 0$ caused by thermodynamic concentration fluctuations was calculated from the concentration dependence of Π_{cr} using eq. 6. The values obtained for $I_{\text{dyn}}(0)$ from osmotic swelling pressure measurements are displayed in the last column of Table 1. These estimates are

Table 1.

Parameters from fits of equation 4 to SANS spectra of 6% (w/w) DNA gels swollen in 100 mM NaCl containing various amounts of CaCl_2 .

$c_{\text{CaCl}_2}/\text{mM}$	$L/\text{\AA}$	$R/\text{\AA}$	m	$I_{\text{dyn}}(0)$ (from SANS)/ cm^{-1}	$I_{\text{dyn}}(0) [= \Delta\rho^2 k_B T \varphi / (\partial\Pi/\partial\varphi)]$ (from osmotic data)/ cm^{-1}
0	16 ± 4	9.7 ± 1	3.2 ± 0.1	0.52 ± 0.09	0.49 ± 0.1
0.2	22 ± 6	9.2 ± 1	3.2 ± 0.1	0.71 ± 0.15	0.69 ± 0.1
0.4	37 ± 8	10.5 ± 1	3.2 ± 0.1	1.21 ± 0.25	1.14 ± 0.2
0.6	68 ± 16	9.6 ± 1	3.2 ± 0.1	2.05 ± 0.42	2.17 ± 0.3
0.8	90 ± 30	10.8 ± 1	3.2 ± 0.1	3.13 ± 0.45	3.27 ± 0.4

in good agreement with $I_{\text{dyn}}(0)$ derived from the fits to the SANS curves. Similar agreement between osmotic and neutron scattering results has been reported previously for neutral polymer gels.^[39–42]

Conclusion

The effect of calcium ions on the larger scale structure of DNA solutions and gels is investigated in near-physiological salt conditions by SANS. Analysis of the SANS response reveals two characteristic length scales, the mesh size L of the transient network, and the cross-sectional radius R of the DNA double helix. The mesh size decreases with increasing DNA concentration as $L \propto c^{-0.73}$. This behavior is similar to that of solutions of flexible neutral polymers, and indicates the loss of spatial correlation as the DNA chains overlap. In gels the mesh size is greater than in the corresponding solutions by approximately 50%. The increase in L reflects the increased heterogeneity of the crosslinked system. The cross-sectional radius of the DNA is practically independent of the polymer concentration and the calcium ion content, and is close to the value of the DNA double helix ($R \approx 10 \text{ \AA}$). This result implies that bundle formation is negligible in the present DNA gels. With increasing calcium chloride concentration both L and the scattering intensity $I_{\text{dyn}}(0)$ arising from thermodynamic concentration fluctuations increase. The latter finding is the consequence of the reduction of the osmotic modulus as the phase transition is approached. The results of this study show that changes in the ionic environment offer a molecular level control of the interactions between DNA strands and allow us to tune the morphology of DNA-based assemblies.

Acknowledgements: This research was supported by the Intramural Research Program of the NICHD, NIH. The authors acknowledge the support of the National Institute of Standards and Technology, U.S. Department of Commerce

for providing access to the NG3 small angle neutron scattering instrument used in this experiment. This work utilized facilities supported in part by the National Science Foundation under Agreement No. DMR-0454672.

- [1] V. A. Bloomfield, *Biopolymers* **1991**, 31, 1471.
- [2] N. V. Hud, M. J. Allen, K. H. Downing, J. Lee, R. Balhorn, *Biochem Biophys Res. Comm.* **1993**, 193, 1347.
- [3] H. Farhood, X. Gao, K. Son, Y. Yang, J. Lazo, L. Huang, J. Barsourn, R. Bottega, R. Eband, *Ann. NY Acad. Sci.* **1994**, 716, 23.
- [4] V. A. Bloomfield, *Current Opinion in Structural Biology* **1996**, 6, 334.
- [5] L. C. Gosule, J. A. Schellman, *Journal of Molecular Biology* **1978**, 121, 311.
- [6] L. M. Santhakumaran, A. Chen, C. K. S. Pillai, T. Thomas, H. He, J. *Nanotechnology in Nonviral Gene Delivery*, Wiley-VCH Verlag GmbH & Co. KGaA, **2005**, p 251–2287.
- [7] G. Lemkine, B. Demeneix, *Current Opinion in Molecular Therapeutics* **2001**, 3, 178.
- [8] J. Lisziewicz, J. Trocio, L. Whitman, G. Varga, J. Xu, N. Bakare, P. Erbacher, C. Fox, R. Woodward, P. Markham, S. Arya, J. P. Behr, F. Lori, *Journal of Investigative Dermatology* **2005**, 124, 160.
- [9] E. R. Toke, O. Lorincz, E. Somogyi, J. Lisziewicz, *International Journal of Pharmaceutics* **2010**, 392, 261.
- [10] O. Lőrincz, E. R. Tóke, E. Somogyi, F. Horkay, P. L. Chandran, J. F. Douglas, J. Szebeni, J. Lisziewicz, *Nanomedicine: nanotechnology, biology, and medicine* **2011**, 8, 487.
- [11] A. Dobi, Dv. Agoston, *Proc. Natl. Acad. Sci. USA*, **1998**, 95, 5981.
- [12] M. Behe, G. Felsenfeld, *Proc. Natl. Acad. Sci. USA*, **1981**, 78, 1619.
- [13] A. Katchalsky, S. Lifson, H. Eisenberg, *J. Polym. Sci.* **1951**, 7, 571.
- [14] K. Yoshikawa, Y. Matsuzama, *Physics D*, **1995**, 84, 220.
- [15] F. Oosawa, *Polyelectrolytes*, Marcel Dekker, New York **1971**.
- [16] R. Kjellander, S. Marcelja, *Chem. Phys. Lett.* **112**, 49, **1984**.
- [17] Y. Zhang, J. F. Douglas, B. D. Ermi, E. J. Amis, *Chem. Phys.* **2001**, 114, 3299.
- [18] I. Morfin, F. Horkay, P. J. Basser, F. Bley, F. Ehrburger-Dolle, A. M. Hecht, C. Rochas, E. Geissler, *Macromol. Symp.* **2003**, 200, 227.
- [19] I. Morfin, F. Horkay, P. J. Basser, F. Bley, A. M. Hecht, P. Rochas, E. Geissler, *Biophys. J.* **2004**, 87, 2897.
- [20] F. Horkay, A. M. Hecht, C. Rochas, P. J. Basser, E. Geissler, *J. Chem. Phys.*, **2006**, 125, 234904.
- [21] M. J. Stevens, *Phys. Rev. Lett.* **1999**, 82, 101.

- [22] M. J. Stevens, *Biophys. J.* **2001**, 80, 130.
- [23] D. W. Yin, F. Horkay, J. F. Douglas, J. J. De Pablo, *J. Chem. Phys.*, **2008**, 129, 154909.
- [24] P. G. de Gennes, *Scaling Concepts in Polymer Physics*, Cornell, Ithaca **1979**.
- [25] L. S. Ornstein, F. Zernicke, *Proc. Sect. Sci. K. med. Akad. Wet.* **1914**, 17, 793.
- [26] F. Horkay, P. J. Basser, A. M. Hecht, E. Geissler, *Macromolecules* **2012**, 45, 2882.
- [27] G. Porod, *Acta Physica Austriaca* **1951**, 2, 133.
- [28] D. Avnir, D. Farin, P. Pfeifer, *Nature* **1984**, 308, 261.
- [29] F. Horkay, P. J. Basser, *Biomacromolecules* **2004**, 5, 232.
- [30] NIST. *Cold Neutron Research Facility NG3 and NG7 30m SANS Instruments Data Acquisition Manual*, Jan **1999**.
- [31] F. Horkay, M. Zrinyi, *Macromolecules* **1982**, 15, 815.
- [32] H. Vink, *Europ. Polym. J.* **1971**, 7, 1411.
- [33] L. R. G. Treloar, *The Physics of Rubber Elasticity*, Clarendon, Oxford **1976**.
- [34] F. Horkay, A. M. Hecht, I. Grillo, P. J. Basser, *J. Chem. Phys.*, **2002**, 117, 9103.
- [35] B. Hammouda, F. Horkay, M. L. Becker, *Macromolecules* **2005**, 38, 2019.
- [36] F. Horkay, P. J. Basser, A. M. Hecht, E. Geissler, *Polymer* **2005**, 46, 4242.
- [37] F. Horkay, P. J. Basser, D. J. Londono, D. A. M. Hecht, E. Geissler, *J. Chem. Phys.*, **2009**, 131, 184902.
- [38] G. Manning, *J. Chem Phys.*, **1969**, 51, 924.
- [39] F. Horkay, A. M. Hecht, S. Mallam, E. Geissler, A. R. Rennie, *Macromolecules* **1991**, 24, 2896.
- [40] F. Horkay, W. Burchard, E. Geissler, A. M. Hecht, *Macromolecules* **1993**, 26, 1296.
- [41] E. Geissler, F. Horkay, A. M. Hecht, *J. Chem. Phys.*, **1994**, 100, 8418.
- [42] F. Horkay, A. M. Hecht, E. Geissler, *Macromolecules* **1998**, 31, 8851.